Monte Carlo simulations for the proton radiography in high-energy-density plasma experiments

Y. Lu[1], H. Li[2], K. Flippo[2], K. Kelso[3], A. Liao[2], S. Li[2], E. Liang[4], P. Tzeferacos[1,5]

[1]Department of Physics and Astronomy, University of Rochester, USA; [2]Los Alamos National Laboratory, USA; [3]Department of Physics, University of Michigan, USA; [4]Department of Physics and Astronomy, Rice University, USA; [5]Laboratory for Laser Energetics, University of Rochester, USA

Abstract

Proton radiography is widely used in high-energy-density (HED) plasma experiments for studying temporal-resolved and spatial-resolved electromagnetic field structures. In some HED plasma experiments, plasma density can play a significant role in diffusing the proton beams and affecting the prediction and interpretation of the proton images. We developed the MPRAD Monte Carlo and ray-tracing code, which can model the deflection of proton beams in arbitrary electromagnetic fields as well as the diffusion of proton beams by Coulomb scattering and stopping power. We use the code as a post-processor to generate synthetic radiographs from static frames in FLASH MHD simulations.

Proton radiography

Proton radiography is a diagnostic tool for temporal-resolved and spatial-resolved studies of the electromagnetic field structures in HED plasmas [1,2], e.g., inertial fusion capsules, magnetic reconnection, self-generated fields, dynamo amplification, etc. Proton image is a two-dimensional mapping of the three-dimensional field distribution. The general mapping can be nonlinear, degenerate and diffusive. Direct interpretation of the proton images is achievable only under the assumptions of simple field geometries. General techniques have been developed to reconstruct the integral quantities over the line of sight, e.g., magnetic field perpendicular to line of sight or MHD current along the line of sight [3-5]. Monte Carlo and ray-tracing methods are used for generating synthetic proton images when the field distribution is preposed by using analytical formulas or postprocessing magnetohydrodynamic or particle-in-cell simulations. Examples of Monte Carlo codes include general-purpose toolkits MCNP [6] and GEANT4 [7], and tools specifically for HED applications [8,9].

MPRAD code

We have developed Monte Carlo and ray-tracing code MPRAD for forward modeling of proton radiography [10]. Proton beam is deflected by electromagnetic field and diffused by Coulomb scattering and stopping power [11]. The flow chart of MPRAD is shown below. MPRAD is written in Python with MPI+OpenMPI parallelization among particles or rays, using Cython and MPI4py package. The Python package yt [12] is used to read the data from FLASH [13] simulations. Precalculated quantities on 3D grid are used to reduce the number of multiplications in the Monte Carlo or ray-tracing calculations.

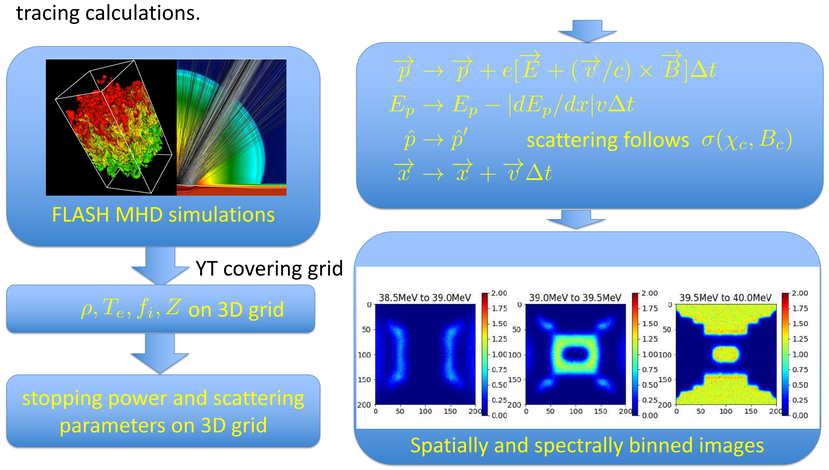

Stopping power

For partially ionized plasma, free electrons, bound electrons, and plasma ions contribute to energy loss of the proton beam. Ignore the usually very small ion contribution, the stopping power $d\langle E_p\rangle/dx$ is given a standard form as [14]

$$\frac{d\langle E_p\rangle}{dx} = -\frac{4\pi e^4}{\beta^2 m_e c^2}\left[n_e f(\beta) + n_b a_b + n_f a_f\right] \quad (1)$$

where $\beta = v_p/c$ is the normalized proton velocity, n_b is the bound electron number density, n_f is the free electron number density, $n_e = n_b + n_f$ is the total electron number density. The function $f(\beta) = \ln[\beta^2/(1-\beta^2)] - \beta^2$ has included the relativistic effect [15]. The value of a_b depends on material property and is given by fitting the PSTAR table [16]. The parameter a_f is given by $a_f = \ln[(m_e^{3/2}c^2)/(\pi^{1/2}\hbar e n_e^{1/2})]$. For Eq (1) to be valid, we need to make a few assumptions: (a) the proton velocity is much larger than the electron velocity, which implies $E_p[\mathrm{MeV}] > (kT_e)/(545\mathrm{eV})$ [17]; (b) the plasma is weakly coupled, whereas in strongly coupled plasmas the model needs to be improved [14] and high-accuracy measurements have been carried out [17]; (c) the beam–plasma coupling can be ignored, which implies $\rho/A \ll 10^4\mathrm{g/cc}$ [19]. The straggling function, i.e., variation of energy loss long the path of motion can be approximated a gaussian distribution [20]. The average square fluctuation in energy loss $\Omega^2 = \langle(\delta E - \langle\delta E\rangle)^2\rangle$ is given by

$$\Omega = \sqrt{4\pi e^4 n_e \frac{1-\beta^2/2}{1-\beta^2} s} = 0.16\mathrm{MeV}\sqrt{\frac{n_e}{10^{23}/\mathrm{cc}}\frac{s}{1\mathrm{cm}}\frac{1-\beta^2/2}{1-\beta^2}} \quad (2)$$

Coulomb scattering

Coulomb scattering of the proton beam in the target is treated by means of the Moliere-Bethe theory of multiple scattering [21]. The distribution of multiple scattering has two parameters χ_c and B_c. The former is given by

$$\chi_c^2 = 4\pi N s e^4 Z(Z+1)/(pv)^2 \quad (3)$$

where p is the proton momentum and v the velocity of the proton beam, N is the number of scattering atoms (or ions) per volume and $s = v\Delta t$ is the path length of the proton beam. B_c is obtained by solving the following equation

$$B_c - \ln B_c = \ln[(\chi_c^2)/(1.167\chi_a^2)] \quad (4)$$

The screening angle χ_a of the partially ionized plasma is [22]

$$\chi_a = (\hbar/p)/\left[a_{TF}^{n_b/n_e} D^{n_f/n_e}\right] \quad (5)$$

where a_{TF} is the Thomas-Fermi screening length due to the bound electrons and D is the Debye length of the plasma. The distribution of the scattering angle θ is expanded in a series of B_c

$$f(z)dz = zdz\left[f^{(0)}(z) + \frac{1}{B_c}f^{(1)}(z) + \frac{1}{B_c^2}f^{(2)}(z) + \cdots\right] \quad (6)$$

where $f^{(n)}(z) = (1/n!)\int_0^\infty u du J_0(zu)\exp(-u^2/4)[(u^2/4)\ln(u^2/4)]^n$ and the normalized scattering angle $z = \theta/(\chi_c B_c^{1/2})$. The first term in Eq (5) is gaussian while the second and third terms are computed at sampled z values for interpolation. We only keep the first three terms, which is sufficient for large B_c. If the value of B_c is small in a timestep, then we fallback to the single Coulomb scattering. The scattering is isotropic in azimuthal direction.

Synthetic proton images and beam deflection in HEDB experiments

Modified Shock-shear targets are used to study self-generated B-field by hydrodynamic instabilities and vortices [23]. The VisRad view on OMEGA and the target are shown below.

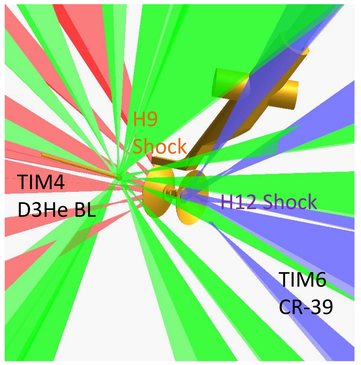

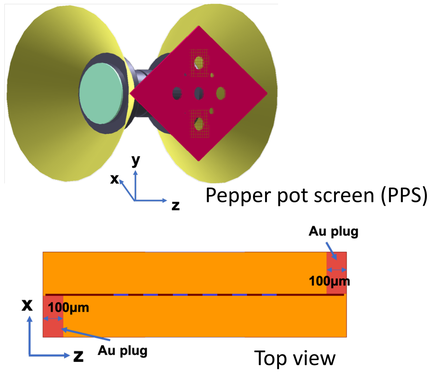

FLASH simulations have been carried out to model the radiation-MHD evolution. As shown below, Biermann battery term generates the magnetic field perpendicular to the x-z plane. Using MPRAD Monte Carlo simulations, we predict that the central blob deflects by ~50μm due to magnetic field.

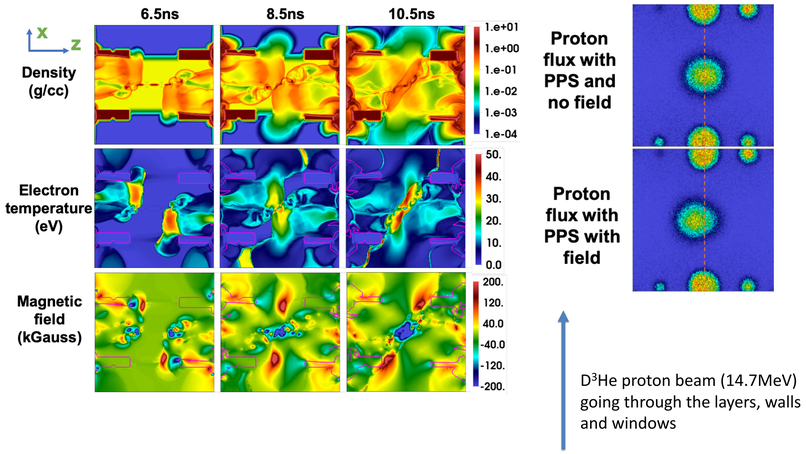

References

[1] Li et al., Phys. Rev. Lett. 97, 135003 (2006).
[2] Borghesi et al., Plasma Phys. Control. Fusion 43 A267 (2001); Zylstra et al., Rev. Sci. Instrum. 83, 013511 (2012).
[3] Kugland et al., Rev. Sci. Instrum. 83, 101301 (2012).
[4] Graziani et al., Rev. Sci. Instrum. 88, 123507 (2017).
[5] Bott, J. Plasma Phys. 83, 905830614 (2017).
[6] Werner et al., LA-UR-18-20808 (2018)
[7] Agostinelli et al., Nucl. Instrum. Methods Phys. Res., Sect. A 506, 250 (2003).
[8] Levy et al., Rev. Sci. Instrum. 86, 033302 (2015).
[9] Volpe et al., IEEE Trans. Plasma Sci. 40, 1131 (2012).
[10] Lu et al., Rev. Sci. Instrum. 90, 123503 (2019)
[11] Manuel et al., Rev. Sci. Instrum. 83, 063506 (2012)
[12] Turk et al., ApJS 192, 9 (2011); https://github.com/yt-project
[13] Fryxell et al., ApJS 131, 273 (2000); Tzeferacos et al., HEDP 17, 24 (2015); http://flash.uchicago.edu
[14] Deutsch et al., Open Plasma Phys. J. 3 88 (2010).
[15] Bloch, Ann. Phys. 16, 285 (1933); Bethe, Z. Phys. 76, 293 (1932); Møller, Ann. Phys. 14, 531 (1932).
[16] https://physics.nist.gov/PhysRefData/Star/Text/PSTAR.html
[17] Li & Petrasso, Phys. Rev. Lett. 70, 3059 (1993).
[18] Zylstra et al., Phys. Rev. Lett. 114, 215002 (2015).
[19] Gericke, Laser Part. Beams 20, 471 (2002).
[20] Lindhard & Sorensen, Phys. Rev. A 53, 2443 (1996).
[21] Moliere, Z. Naturforsch., A 3, 78 (1948); Bethe, Phys. Rev. 89, 1256 (1953).
[22] Nardi et al., Laser Part. Beams 25, 489 (2007).
[23] Lu et al., Phys. Plasmas 26, 022902 (2019).

We acknowledge support by the LANL-LDRD program 20180040DR and DOE NNSA grant No. DE-NA0003942 and DE-NA0002721. The research and materials were partially developed at the National Laser Users' Facility (NLUF) at the University of Rochester's Laboratory for Laser Energetics (LLE), with financial support from the U.S. DOE under DE-NA0001944. Proton radiography was supported in part by U.S. DOE grants DE-FG03-09NA29553 and DE-SC0007168. The simulations were performed with LANL Institutional Computing supported by the U.S. DOE NNSA under Contract No. 89233218CNA000001, and with the Extreme Science and Engineering Discovery Environment (XSEDE) supported by National Science Foundation (NSF) grant number ACI-1548562. The Flash Center for Computational Science acknowledges support from the U.S. DOE NNSA under Subcontract No. 536203 with Los Alamos National Laboratory, Subcontract B632670 with Lawrence Livermore National Laboratory, and Award Numbers DE-NA0003842 and DE-NA0003934. We also acknowledge support from NSF Award Number PHY-2033925.